Granulite-facies contact metamorphism around the Hakefjorden Norite-Anorthosite Complex, SW Sweden

Hans Årebäck & Ulf B. Andersson

Årebäck, H & Andersson, U.B.: Granulite-facies contact metamorphism around the Hakefjorden Norite-Anorthosite Complex, SW Sweden. *Norsk Geologisk Tidsskrift*, Vol. 82, pp. 29-44. Trondheim 2002. ISSN 029-196X.

Granulite-facies contact metamorphic mineral assemblages developed in the aureole of the ca. 916 Ma Hakefjorden norite-anorthosite complex, SW Sweden. Outside the immediate contact, country rocks consisting of Mesoproterozoic meta-greywackes preserve a pre-intrusive, regional amphibolite-facies mineral assemblage of quartz, plagioclase, K-feldspar, biotite, muscovite, and scarce garnet. Several reactions at the immediate contact produced high-temperature assemblages comprising sillimanite, cordierite, orthopyroxene, high-temperature garnet rims, corundum, hercynitic low-Zn spinel, K-feldspar, and melt. Considerable changes in the composition of biotite and plagioclase also occurred. The pre-existing amphibolite-facies assemblage was recrystallised, partially consumed, or partially molten. Garnet porphyroblasts show preserved prograde growth zoning with strongly increasing pyrope content in the outermost rims. In other instances, rims are resorbed, contributing to the formation knot-like, SiO_2-deficient intergrowths of cordierite + spinel + sillimanite +K-feldspar + plagioclase ± corundum. Textural and compositional heterogeneity indicates that equilibrium conditions were attained only on a local mm-size scale. Some of the garnet appears to preserve a zoning record of two pre-intrusive metamorphic growth episodes. Geothermobarometry of assemblages in local textural equilibrium records low-P, ultra-high-T granulitic peak contact metamorphic conditions of 890-1015°C at pressure below 6 kbar.

Hans Årebäck, Department of Geology, Earth Sciences Centre, Göteborg University, Box 460, SE-405 30 Göteborg, Sweden. Present address: Noréns väg 3, SE-936 32 Boliden, Sweden. e-mail: hans.areback@boliden.se
Ulf B. Andersson, GeoForschungsZentrum, P.B. 4.1, Telgrafenberg, D-14473 Potsdam, Germany. Present address: Laboratory for Isotope Geology, Swedish Museum of Natural History Box 50007, SE-10405 Stockholm. e-mail: ulf.andersson@nrm.se

Introduction

Accurate pressure and temperature estimates are crucial to our understanding of intrusions particularly because these data constrain the depth of emplacement. Well-developed aureoles in favourable rock types may contain metamorphic mineral assemblages equilibrated during the thermal peak and thus yield information on the physical conditions of intrusion. Partial melting and granulite-facies assemblages in contact metamorphic aureoles around mafic intrusions have been widely described in the literature (e.g. Loomis 1972; Berg 1977; Grant & Frost 1990; Owen 1991; Dasgupta et al. 1997). They are characterised by high-temperature mineral assemblages formed at T ≥700°C (e.g. Srogi et al. 1993). Typical assemblages in metapelitic rocks close to the contacts in low- to intermediate-pressure aureoles comprise garnet + cordierite + spinel + orthopyroxene + sillimanite + K-feldspar + plagioclase + quartz + melt ± corundum (e.g. Pattison & Tracy 1991; Dasgupta et al. 1997, and references therein), and sometimes the ultra-high temperature (>900°C) mineral osumilite (Harley 1996, and references therein). Cordierite-spinel assemblages are common in high-grade contact metamorphic aureoles and have been referred to as cordierite-spinel knots (e.g. Loomis 1972; Berg 1977; Grant & Frost 1990).

In this paper, we report data from the contact aureole around the late Sveconorwegian norite-anorthosite Hakefjorden Complex (HFC), SW Sweden, in which mineral assemblages suggest formation during low- to intermediate-pressure granulite conditions. Osumilite, or pseudomorphs after it, has not been observed, although the calculated P-T conditions are within its stability field. Instead, formation of knot-like intergrowths of cordierite + spinel + sillimanite ± corundum is typical, which has also been reported from several contact aureoles (Grant & Frost 1990; Owen 1991; Dasgupta et al. 1997).

Geological setting

The HFC was described in detail by Årebäck (1995; 2001) and Årebäck & Stigh (1997; 2000). It consists of a norite/monzonorite intrusion carrying abundant blocks of anorthosite (2 cm to 50 m in size), situated about 25 km NNW of Göteborg, SW Sweden (Fig. 1). It forms two east-west elongated bodies, both about 500 m wide and 3.6 and 1.2 km long respectively, intruding Mesoproterozoic meta-greywacke of the Stora Le-Marstrand Formation (SLM; Fig. 1). The SLM consists of alternating quartzo-feldspathic and pelitic units with

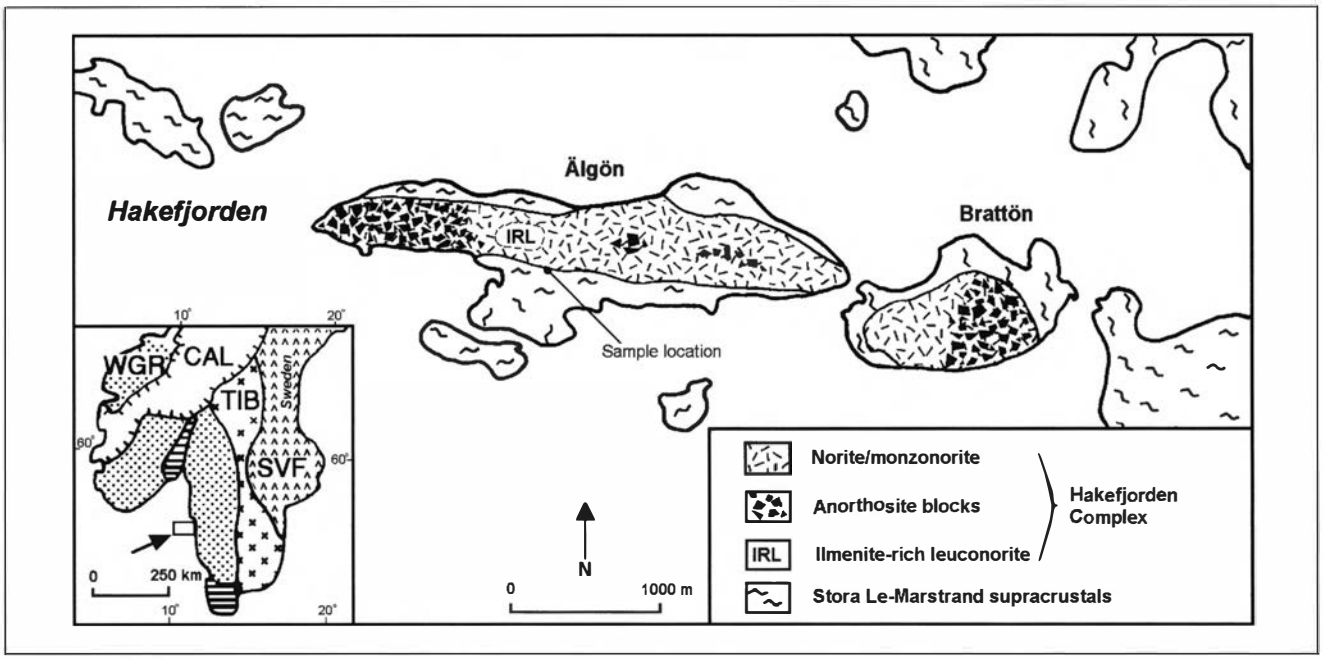

Fig. 1. Simplified geological map of the Hakefjorden Complex and surrounding rocks (after Årebäck & Stigh, 1997), with sample location. The inset map shows the major lithotectonic units of southwestern Fennoscandia. CAL = Caledonian; SVF = Svecofennian; TIB = Transscandinavian Igneous Belt; WGR = Western Gneiss Region; dotted areas = rocks affected by the Sveconorwegian Orogeny; ruled areas = Phanerozoic rocks.

local occurrences of calc-silicates. It is metamorphosed in the amphibolite facies and typically contains quartz, plagioclase, K-feldspar, biotite, muscovite, and scarce garnet (Bergström 1963; Sigurdsson 1990; Austin Hegardt 2000; Eliasson et al., in prep.). According to Åhäll et al. (1990; 1998), amphibolite-facies metamorphism and migmatization in SLM is related to Gothian (ca. 1.75-1.55 Ga) regional deformation, while later Sveconorwegian deformation (1.1-0.9 Ga) is mostly restricted to shear zones and folding. Whole-rock K-Ar dating of SLM rocks situated two kilometers south of HFC yielded ages of 1.07-1.04 Ga, interpreted to date a metamorphic event (Magnusson 1960).

P-T estimates of two samples from the SLM, a garnet-bearing amphibolite and a garnet-bearing leucosome in the meta-greywakes about 5.5 km and 4 km south of the HFC, respectively, suggest regional metamorphic conditions of around 7-8 kbar and ~620°C (Austin Hegardt 2000). Preliminary geothermobarometric estimates from garnet- and quartz-bearing calc-silicate lenses in SLM meta-greywakes ca. 80 km NNE of the HFC indicate that the last metamorphism (Sveconorwegian?) reached at least 5-7 kbar, and 500-550°C (Sigurdsson 1990).

The HFC shows no signs of ductile deformation and is discordant to the metamorphic fabric of the SLM. A 5-20 m wide partially melted contact aureole that commonly disrupts the earlier regional migmatite structures, has developed around the intrusion. Recent U-Pb geochronology of zircons from the contact melt (leucosome) yields an age of 916 ± 11 Ma, interpreted to represent the minimum crystallisation age of HFC (Scherstén et al. 2000). The melanosome of the contact aureole contains plagioclase, quartz, garnet, cordierite, K-feldspar, orthopyroxene, biotite, spinel, sillimanite, and corundum.

Samples and analytical techniques

Samples for polished thin sections were collected at the immediate intrusion contact, central Älgön (Fig. 1). A few samples at 10-20 m distance from the intrusion and

Fig. 2. Contact migmatite developed in the Stora Le-Marstand metasediment at the immediate intrusion contact showing the chaotic orientation of foliated fragments and quartz veins, eastern Älgön. In the lower right part of the photography norite (dark) with blocks of anorthosite (light grey) occurs.

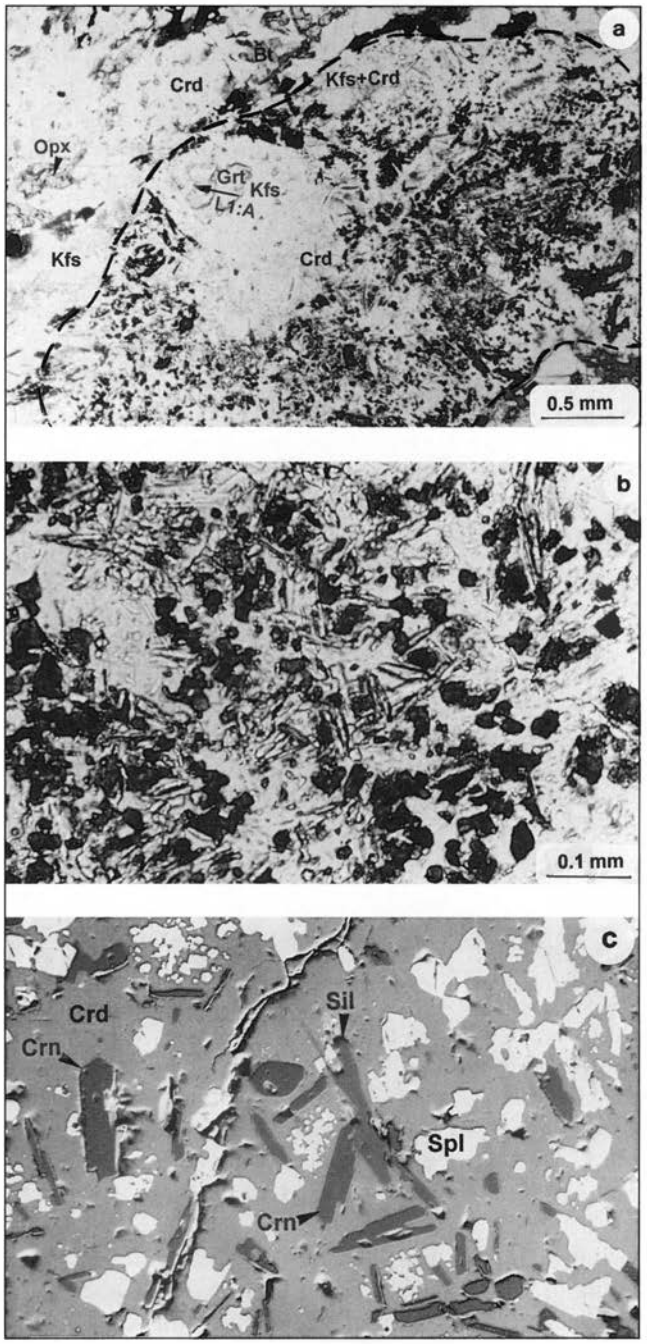

Fig. 3. Photomicrographs (a) and (b), and back-scattered electron (BSE) image (c) of a cordierite-spinel knot in sample L1. (a) Garnet (Grt) and K-feldspar (Kfs) occur in the upper left part of the knot. In addition to cordierite (Crd) and spinel (dark), the knot consists of moderate contents of sillimanite (needel-shaped mineral) and minor plagioclase and corundum (not visible). The broken line represent the outer limit of the knot; location of compositional profile L1:A is shown. Matrix phases present outside the knot are K-feldspar (Kfs), cordierite (Crd), orthopyroxene (Opx), biotite (dark), and minor quartz. Plane-polarised light. (b) Close-up of the knot showing cordierite (matrix), spinel (dark), sillimanite and corundum (needle-shaped). Plane-polarised light. (c) Back-scattered electron image showing spinel (Spl), sillimanite (Sil) and corundum (Crn) in a matrix of cordierite (Crd).

a few SLM samples not affected by contact metamorphism have been examined too, but not analysed for mineral chemistry.

Microprobe analyses were obtained with a Cameca Camebax SX50, Department of Earth Science, Uppsala University. Operating conditions were 20 kV accelerating voltage, 15 nA beam current, 1-2 μm beam diameter, with counting times of 10-25 s (depending on the element). Calibration was performed on natural and synthetic mineral standards from Cameca. Compositional profiles through minerals reported in Figs. 6 and 7b are based on complete spot analyses.

Petrography and mineral chemistry

The present study concentrates on well-preserved peak metamorphic assemblages in the HFC contact aureole melanosome, focusing on petrological indicators for P-T conditions. The HFC induced partial melting in the SLM metasediments that resulted in anatectic, granitic veins and dykes which sometimes back-vein the HFC (Årebäck 1995). In places, the contact migmatites have a spectacular appearance with a chaotic disruption of the SLM-foliation and abundant quartz veins oriented in different directions (Fig. 2). However, on the centimetre-scale, the melanosome is a rather massive hornfels. The granitic veins and dykes (leucosome) are fine- to medium-grained, equigranular, and consist essentially of quartz, K-feldspar, albite, and subordinate chlorite (Årebäck 1995; Cornell et al. 2000). Accessory minerals include apatite, muscovite, hematite, zircon, sphene, and epidote.

The hornfels at the immediate contact is fine- to medium-grained and has a granoblastic to porphyroblastic texture. Garnet and cordierite occur as porphyroblasts. Two samples (2A and L1) have been investigated for mineral chemistry and P-T estimates. In sample 2A the porphyroblastic garnet is weakly or moderately resorbed and surrounded by abundant, small pods of quartz, recrystallised feldspars, and minor biotite. In sample L1, cordierite + spinel + sillimanite ± corundum ± K-feldspar ± plagioclase form symplectites occurring as irregular, up to 5 mm wide domains, the cordierite-spinel knots (Fig. 3). In places, these cordierite-spinel knots contain small, anhedral to subhedral garnet in their central parts (Fig. 3a). These garnets are interpreted as remnants of larger garnets that have been extensively replaced by cordierite + plagioclase (An_{42-47}) ± K-feldspar, grading outwards to cordierite + spinel + sillimanite + progressively more Ca-rich plagioclase (An_{52-61}) ± corundum symplectites. The hornfels matrix consists essentially of cordierite, K-feldspar, biotite, orthopyroxene, plagioclase, and quartz. Ilmenite, Fe-sulphides, and zircon occur in minor amounts. In

the best-preserved rocks (e.g. sample L1), the contact metamorphic high-grade assemblages are pristine. In other samples (e.g. sample 2A) they have been considerably retrogressed, with cordierite partly altered to a mass of fine-grained white mica (pinnite), biotite locally replaced by secondary chlorite, orthopyroxene by secondary biotite, and plagioclase may show some sericitisation.

In this study, the assemblages more than 1 metre from the intrusion have not been analysed for mineral chemistry. However, a few samples collected 10 to 20 metres from the intrusion, have been studied petrographically. In these, the contact metamorphic assemblage consists of discrete grains of altered cordierite and 0.5-5 mm wide irregular domains of fibrolitic and prismatic sillimanite intergrown with biotite and K-feldspar, in places mantled by spinel ± cordierite.

Garnet

Garnet occurs both as 'small' (0.1-1 mm), anhedral to subhedral grains in the matrix and 'large' (0.5-2.5 mm), subhedral, rounded porphyroblasts (Fig. 4, 5). The large grains contain abundant inclusions of plagioclase (An_{20-55}), some quartz, and rare biotite in the cores and intermediate zones. The rims are almost inclusion-free. Garnet zoning profiles were obtained from three large garnets (two rounded and one irregular) in contact with plagioclase, quartz, cordierite, and biotite (Fig. 5a-c, 6b-d) and one small garnet in contact with K-feldspar and cordierite inside a cordierite-spinel knot (Fig. 3a, 6a).

Porphyroblastic garnet. – The garnet porphyroblasts show prograde growth zoning with rimward increasing pyrope content, decreasing Fe/(Fe+Mg) ratio, and decreasing spessartine content (Fig. 6). Three different zones can be distinguished. Cores, which occur only in some porphyroblasts (possibly due to off-centre sections), have fewer inclusions that are commonly oriented in straight trails, compared to the intermediate zones. The latter are rich in inclusions (mainly plagioclase ± quartz) oriented in a concentric fashion (Fig. 5b-c). The outermost rims are essentially inclusion-free. The cores are rich in grossular and spessartine components (X_{Grs} up to 20, and X_{Sps} up to 38). The intermediate zones generally show smooth zoning patterns with decreasing X_{Grs} and X_{Sps}, and Fe#, while X_{Alm} and X_{Prp} increase (Fig. 6d). The outermost rims are associated with a strong increase in X_{Prp} (up to 29). In one case a high pyrope plateau (about 45 µm wide) has developed along the margin (Fig. 6c). This plateau has a very gentle slope with increasing Fe# towards the garnet edge. All three garnet porphyroblasts analysed occur in the same garnet-rich sample, 5-15 mm from each other. Cordierite in contact with these porphyroblasts is interpreted to have replaced the rims of garnet (Fig. 5d).

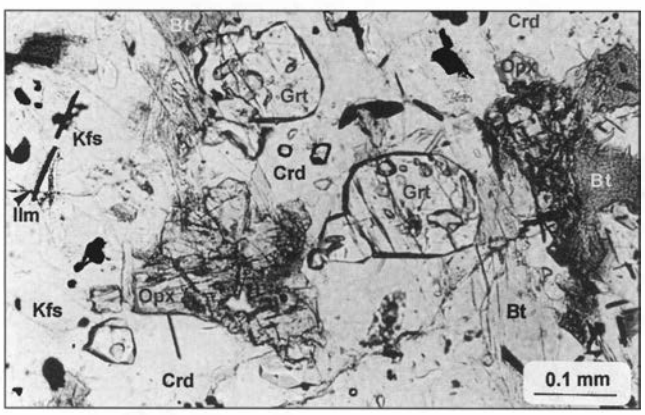

Fig. 4. Photomicrograph of the matrix phases including garnet (Grt), cordierite (Crd), K-feldspar (Kfs), biotite (Bt), orthopyroxene (Opx), ilmenite + Fe-sulphides (black), and minor interstitial quartz. Plane-polarised light. Sample L1.

Matrix garnet and garnet within cordierite-spinel knots. – These are more anhedral than the garnet porphyroblasts. Inclusions are less common and no regular zoning has been observed. They are dominantly almandine (64-76 mol%), with 7-11 mol% spessartine, 11-25 mol% pyrope, and 3-5 mol% grossular. Garnet within the cordierite-spinel knots is anhedral and displays a very homogeneous composition (Fig. 6a).

Cordierite

Cordierite occurs both as euhedral, tabular and rounded porphyroblasts (0.2-2 mm; sample 2A; Fig. 7a), subhedral to anhedral grains in the matrix, and as cordierite-spinel knots (<0.5 to 5 mm) with intergrowths of spinel ± sillimanite ± plagioclase ± corundum (sample L1; Fig. 3). The cordierite is believed to be of contact metamorphic origin, since it to our knowledge has not been reported from elsewhere in the SLM. Sector twinning is common (Fig. 7a) and pinnitisation occurs along grain boundaries and microcracks. Compositional variations between cordierites in different textural positions are distinct, but only minor zoning in single grains or single domains has been observed (cf. Fig. 7b). Fe/(Fe+Mg) ratios of matrix cordierite in sample L1 vary from 43 to 46, while cordierite in the cordierite-spinel knots within the same sample are distinctly more Fe-rich (Fe# = 51-56). In sample 2A, a few metres from sample L1, only porphyroblastic cordierites have been analysed, having Fe/(Fe+Mg) ratios from 29 to 36. A profile across a round porphyroblast (Fig. 7) displays a slight increase of Fe# in the outermost rim.

Plagioclase and K-feldspar

Plagioclase grains are typically subhedral to anhedral and irregular. A patchy texture comprising compositionally different plagioclase phases and irregular quartz

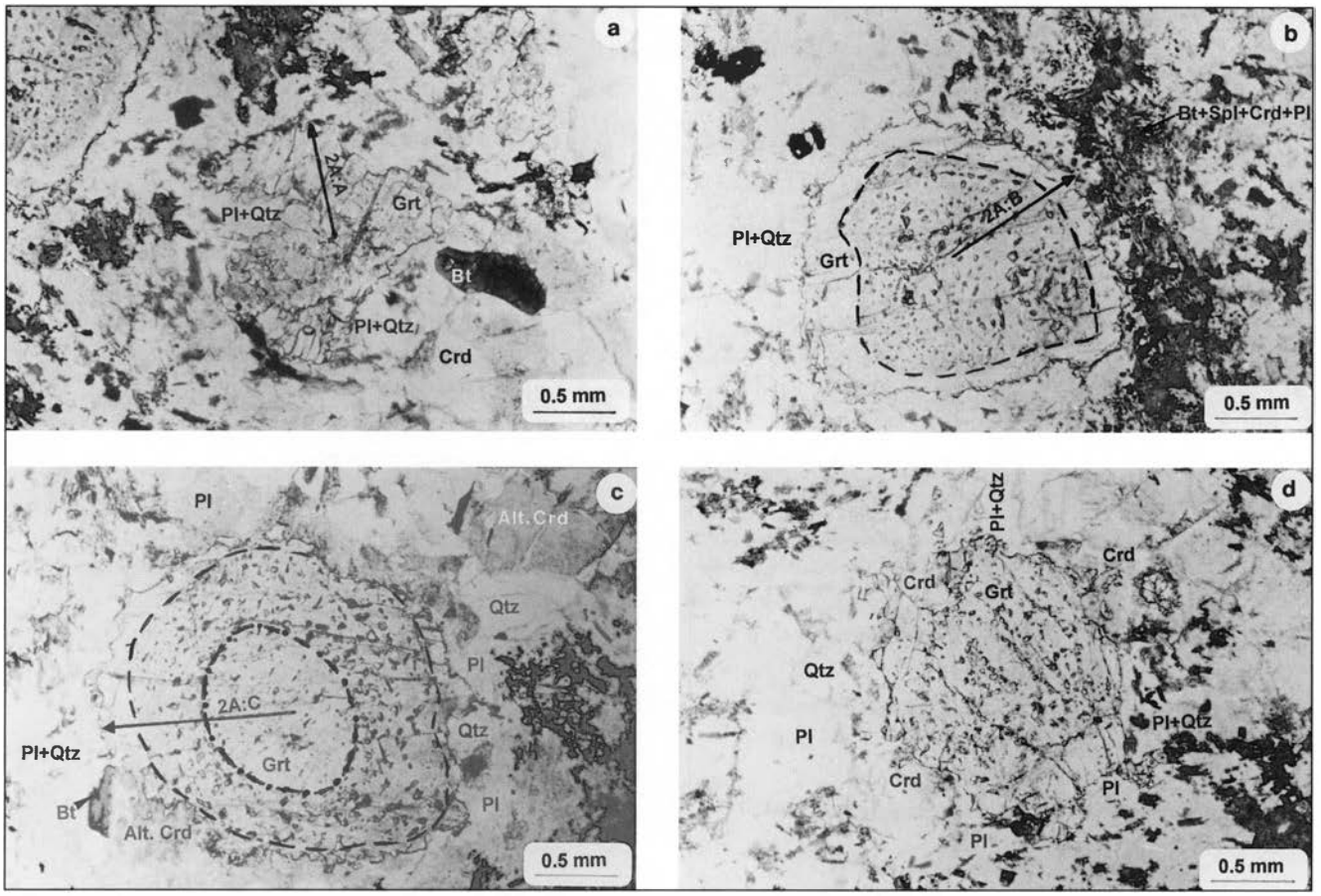

Fig. 5. Photomicrographs showing garnet porphyroblasts (Grt) and associated phases, plagioclase (Pl), biotite (Bt), cordierite (Crd), and spinel (Spl), in sample 2A, and the location of garnet compositional zoning profiles. Plane-polarised light. (a) Compositional zoning profile 2A:A. (b) Compositional zoning profile 2A:B; broken line represents the approximate transition between the intermediate zone and the rim. (c) Compositional zoning profile 2A:C; broken line with dots represents the approximate transition between the core and the intermediate zone; broken line represents the approximate transition between the intermediate zone and the rim. (d) Garnet porphyroblast in contact with plagioclase (Pl), quartz (Qtz), biotite (dark), and cordierite (Crd). The latter is suggested to partly replace garnet. Note the irregular embayments of the garnet.

inclusions is frequent, particularly in sample 2A (Fig. 8). In these grains the outer zone is in general more Na-rich (An_{25-28}) than the core (An_{36-39}; Table 1). Matrix plagioclase, which does not show this patchy texture, varies from An_{20} to An_{33} (average $An_{27.5}$). Plagioclase within cordierite-spinel knots occurs as irregular grains with a progressive increase in anorthite component from the centre (An_{42}) and outwards (to An_{61}). Inclusions of plagioclase within garnet vary in composition from An_{52} to An_{55} in the relatively grossular-rich (Fig. 5c), and from An_{19} to An_{30} in the relatively grossular-poor garnets (Fig. 5b).

K-feldspar occurs both in the matrix, in sample L1 associated with orthopyroxene, cordierite, and biotite, and as larger grains associated with cordierite-spinel knots. The latter have a composition of Or_{73-76} Ab_{23-26}.

Biotite, orthopyroxene and ilmenite

Biotite is abundant in the matrix, but is absent from the cordierite-spinel knots. In general, it is reddish and strongly pleochroic in the contact aureole and brown to greenish brown outside the aureole. The TiO_2 content of biotites in the contact aureole is typically high (3.0-5.7 wt%), and their Fe# vary from 46 to 60. Although generally fresh, some alteration to chlorite ± muscovite ± rutile is observed. A single biotite inclusion from a garnet porphyroblast ranges in Fe# from 57 to 58.

Orthopyroxene replaces biotite and is abundant in biotite-rich domains (Fig. 9). In sample L1, the enstatite component ranges from 38 to 41, and in sample 2A from 45 to 47, except in a small orthopyroxene inclusion within a cordierite porphyroblast (Fig. 7; Table 2) in which the most Mg-rich composition, En_{52}, is recorded. The orthopyroxenes are moderately aluminous with Al_2O_3 ranging from 1.5 to 4 wt%.

Small, 0.01-0.2 mm long, needle-shaped or rounded ilmenite grains occur, particularly together with feldspars, orthopyroxene, and cordierite (possibly replacing biotite). They are almost end-member ilmenites with X_{Ilm} from 0.92 to 0.96 and $X_{Pyrophanite\ (Py)}$ =0.03-0.08.

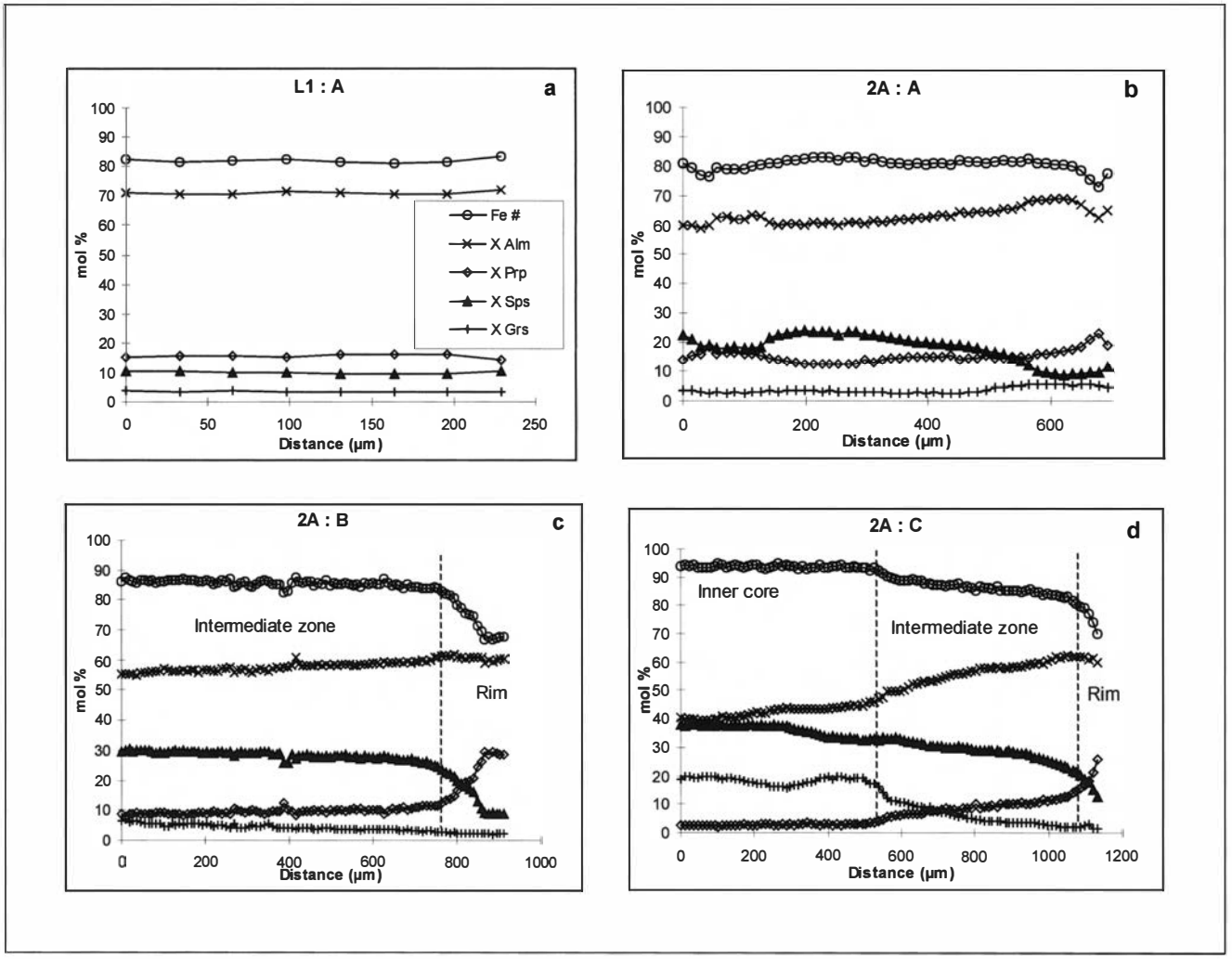

Fig. 6. Compositional zoning profiles of garnets, for locations see Fig. 3 and 5. (a) Across a garnet occurring in a cordierite-spinel knot, L1:A. (b) From core to rim of an irregular porphyroblast, 2A:A. Note the slight increase of X_{Sps} in the outermost rim which may indicate resorption. (c) From core (intermediate zone) to rim of a rounded porphyroblast, 2A:B. Note the strong increase of X_{Prp} in the rim and ca. 45 µm wide high Mg-plateau in the outer rim. (d) From core to rim of a rounded porphyroblast, 2A:C, which display the compositional differences between the core (relatively high in X_{Grs}), intermediate zone, and rim (strong increase in X_{Prp}).

Spinel

Spinel occurs as microscopic (ca. 10-100 µm), equidimensional to needle-shaped, dark green grains, predominately in symplectitic intergrowths within cordierite (Fig. 3), but also as minute grains within plagioclase. In sample 2A, spinel is also observed together with quartz. All grains are hercynitic in composition with Fe/(Fe^{2+}+Mg) ratios of 74-91, Al/(Al+Cr+Fe^{3+}) ratios of 96-99 and Zn-contents from 0.18 to 0.76 wt% ZnO (average 0.42 wt% ZnO; Table 2).

Sillimanite and corundum

Sillimanite has been observed at the immediate intrusion contact only as intergrowths within cordierite-spinel knots (sample L1 & 2A; Fig. 3). Further away from the contact (ca. 10-20 m) elongate domains of fibrolitic and prismatic sillimanite are intergrown with biotite and K-feldspar (sample 92046; Fig. 10), in places with a rim of intergrown spinel + cordierite. The sillimanite in the cordierite-spinel knots contains minor amounts of iron (Fe_2O_3 =0.6-1.6 wt%; Table 2).

Small amounts of fine-grained corundum occur in places in the cordierite-spinel knots. It is prismatic to needle-shaped and because of the small size (ca. 10-80 µm), very hard to distinguish from sillimanite and impossible to detect without backscatter imaging (Fig. 3c). Corundum occurs together with spinel, sillimanite ± Ca-rich plagioclase in the outer half of the cordierite-spinel knots. Three analyses indicate minor amounts of iron (Fe_2O_3 0.4-0.7 wt%; Table 2).

Discussion

Textural interpretation and reaction history

In the HFC aureole, newly formed contact metamorphic minerals comprise sillimanite, cordierite, orthopy-

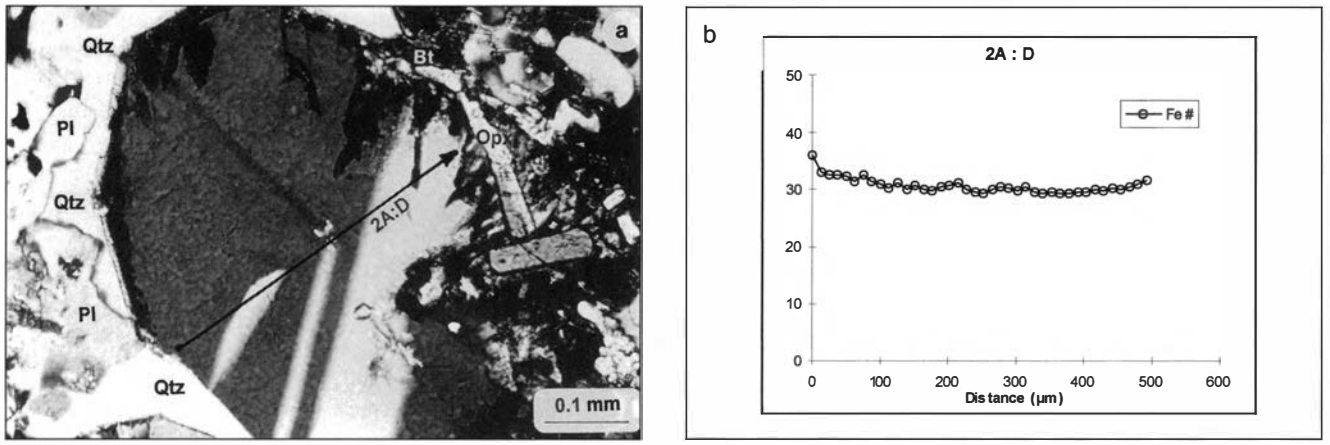

Fig. 7. (a) Photomicrograph of cordierite porphyroblast in contact with quartz (Qzt), plagioclase (Pl), biotite (Bt), and orthopyroxene (Opx). Location of the compositional profile 2A:D. Plane-polarised light. Sample 2A. (b) Compositional zoning profile across the cordierite porphyroblast shown in (a).

roxene, corundum, and hercynitic spinel, while minerals of the pre-existing SLM amphibolite-facies assemblage (quartz, plagioclase, biotite, muscovite, K-feldspar, and garnet) have been strongly affected by the contact metamorphism. Biotite, quartz, plagioclase, and garnet were partially consumed and muscovite disappeared completely. New formation of K-feldspar, melt (Kfs + Qtz + Na-rich Pl), and garnet, as well as considerable changes in the composition of biotite and plagioclase are observed. The systematic variation in plagioclase composition within and among samples is consistent with incongruent melting, and partitioning of an albite-rich component into granitic melt leaving a more calcic plagioclase in the residue.

The fact that cordierite has not been reported from the regional amphibolite-facies metasedimentary rocks may be attributed to several factors. Firstly, the estimated pressure-temperature conditions for the regional metamorphism (ca. 6-8 kbar at ca. 550-650°C; Sigurdsson 1990; Austin Hegardt 2000) exceed the stability field with respect to pressure for pure Mg-cordierite (Bucher & Frey 1994, and references therein). Secondly, for systems richer in Fe, cordierite stability is restricted to even lower pressures. Thirdly, the SLM metasediments are in general not particularly Al-rich, suppressing the formation of Al-rich silicates that could contribute to the low abundance of garnet, and absence of aluminium silicates and staurolite.

Rocks 10-20 m from the intrusion contact. – Formation of sillimanite intergrown with K-feldspar and biotite can be described by the breakdown and disappearance of muscovite according to the reaction (e.g. Pattison & Tracy 1991):

$$Ms + Pl + Qtz = Sil + Kfs + melt \quad (1)$$

Reaction (1) occurs some tens of degrees higher than the beginning of H_2O-saturated melting in pelitic rocks, which takes place at c. 650°C at pressures >3.9 kbar according to (e.g. Pattison & Tracy 1991):

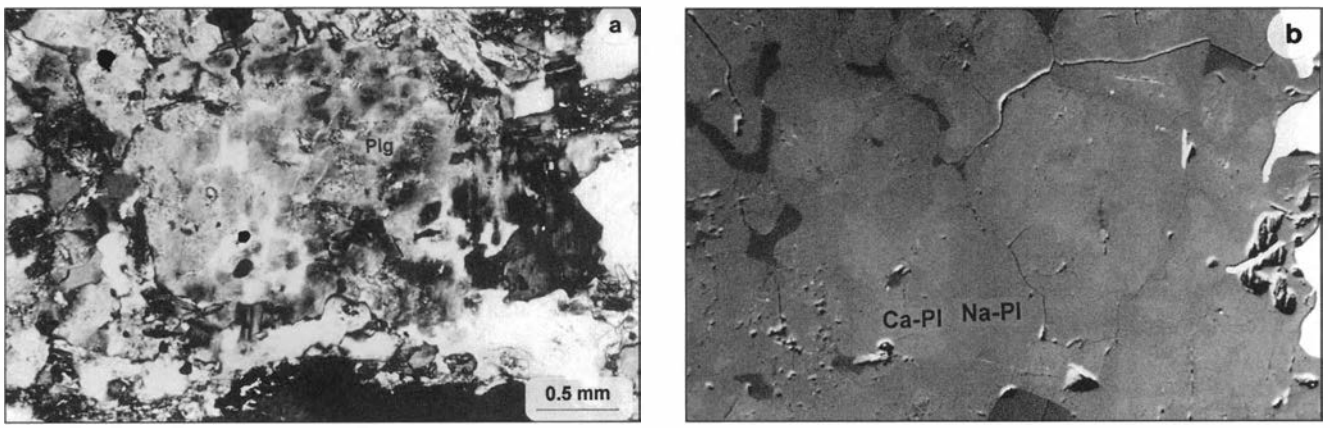

Fig. 8. (a) Photomicrograph (crossed polarisers) and (b) BSE image of cellular plagioclase (Pl) in sample 2A. In the BSE image lighter grey areas, mainly in the core of the grains, represent more Ca-rich plagioclase (Ca-Pl) than darker grey areas (Na-Pl).

$$Ms + Qtz + Pl + H_2O = melt\ (precipitating\ mainly\ Kfs + Pl + Qtz) \quad (2)$$

In some margins of the sillimanite + K-feldpar ± biotite intergrowths, cordierite + spinel has started to grow, suggesting the reaction (e.g. Srogi et al. 1993; Dasgupta et al. 1997):

$$Bt + Sil + Qtz = Spl + Crd \pm Kfs + melt \quad (3)$$

Rocks at the immediate intrusion contact (<1 m). – At the contact, the cordierite-spinel knots are extensively developed, suggesting that the above reaction (3) has gone to local completion. Spinel-cordierite assemblages are common in pelitic rocks metamorphosed at low pressure and high temperature (e.g. Dietvorst 1980; Montel et al. 1986; Grant & Frost 1990; Clarke et al. 1990; Owen 1991; Srogi et al. 1993; Fitzsimons 1996; Dasgupta et al. 1997; Whittington et al. 1998; Li & Naldrett 2000; Scrimgeour et al. 2001).
The formation of the contact metamorphic pyrope-rich garnet may have occurred as a new growth rim on the regional metamorphic grains according to (Pattison & Tracy 1991, and references therein):

$$Bt + Sil + Qtz + Pl = Crd + Grt + Kfs + melt \quad (4)$$

The cordierite and garnet porphyroblasts in sample 2A are typically surrounded by leucocratic coronas consisting mainly of quartz and plagioclase with some biotite. These coronas represent the melt formed, and here the plagioclase commonly shows a patchy, cellular compositional zoning indicative of partial melting (Fig. 8). Locally in the aureole, garnet was also consumed according to reactions (5) and (10) (see below).
The remnants of corroded garnets inside some of the cordierite-spinel knots suggest that garnet was also consumed during the formation of at least some of these knots (cf. e.g. Srogi et al. 1993; Fitzsimons 1996; Dasgupta et al. 1997) possibly according to a reaction of the type:

$$Grt + Bt + Sil + Qtz = Crd + Spl \pm Kfs + melt \quad (5)$$

The remnants of garnet and sillimanite may indicate that reaction (5) stopped when biotite was consumed. If low in the gahnite component, as here, spinel is stable together with quartz in metapelitic rocks at a minimum temperature of 800° C at about 3 kbar, while breaking down to garnet + sillimanite at higher, and cordierite at lower pressures (Montel et al. 1986; Waters 1991). However, in some knots, local SiO_2-undersaturated conditions seem to have prevailed following the consumption of quartz, facilitating the formation of corundum together with spinel (e.g. Srogi et al. 1993):

$$Bt + Sil = Crd + Spl + Crn + melt \quad (6)$$

This may be due to centimetre-scale, pre-existing compositional heterogeneities in the SLM migmatites, which enhanced by partial melt removal resulted in the quartz-depleted domains. Corundum within cordierite + spinel domains is described by Srogi et al. (1993) from granulite-facies gneisses, where in some samples the corundum is in apparent textural equilibrium with cordierite + spinel + garnet, whereas textures in other samples suggest growth of sillimanite and spinel at the expense of corundum and cordierite. Corundum may also be produced by the breakdown of plagioclase according to (Li & Naldrett 2000):

$$Na\text{-}Ca\ Pl = Crn + Anorthite + melt\ (Na_2O + SiO_2) \quad (7)$$

The fact that corundum is associated with the most Ca-rich plagioclase (An_{52-61}) recorded in the investigated samples, and the progressive increase in anorthite content of plagioclase from the centre of the cordierite-spinel knots toward their margin may support that reaction (7) has occurred. The co-existence of cordierite, spinel and corundum suggests pressures less than ca. 6 kbar (Hensen 1987).

In the contact aureole (pelitic rocks) around the Laramie anorthosite complex, mineral assemblages similar to those described here occur (Grant & Frost 1990). Amongst others, the association of prismatic sillimanite and corundum in a matrix of cordierite + hercynitic spinel + K-feldspar is also found very close to the contact. Grant and Frost (1990) proposed that the association of sillimanite and corundum may represent pseudomorphs after mullite. However, no indication of mullite has been detected in the studied samples.

Orthopyroxene typically occurs as grains replacing biotite, suggesting the dehydration-melting of biotite to be the major pyroxene-forming reaction (e.g. Waters 1988, Andersson et al. 1992, Bégin & Pattison 1994 and references therein):

$$Bt + Pl + Qtz = Opx + Kfs + melt \quad (8)$$

Cordierite occurs in textural equilibrium with orthopyroxene, the latter also as inclusions in the cordierite in

the quartz-rich domains. Moreover, small grains of garnet commonly occurs as inclusions in cordierite and associated with biotite, orthopyroxene and K-feldspar (Cf. Fig. 4). This may indicate that garnet was consumed in an orthopyroxene + cordierite + K-feldspar-forming reaction. These observations suggest that the following reactions may be appropriate (e.g. Pattison & Tracy 1991):

$$\text{Bt} + \text{Qtz} = \text{Opx} + \text{Crd} + \text{Kfs} + \text{melt} \quad (9)$$

$$\text{Bt} + \text{Grt} + \text{Qtz} = \text{Opx} + \text{Crd} + \text{Kfs} + \text{melt} \quad (10)$$

To summarise, a generalised continuous reaction of the form:

$$\text{Bt(1)} + \text{Qtz} + \text{Grt(1)} + \text{Pl(1)} \pm \text{Sil} = \text{Crd} + \text{Spl} \pm \text{Crn} + \text{Bt(2)} + \text{Grt(2)} + \text{Pl(2)} + \text{Kfs} + \text{melt} \quad (11)$$

is proposed for the HFC contact event. Phases labelled (1) refer to pre-existing regional metamorphic phases and those labelled (2) to phases recrystallised as a result of the HFC intrusion. The strong increase of the pyrope-content in the outer rims of the garnet porphyroblasts indicate high-temperature growth, in agreement with their proposed development during the HFC contact metamorphism (Grt(2)). The core and intermediate zone of the garnets were formed during previous regional metamorphism (Grt(1)).

Disequilibrium and local equilibrium

The textures observed in the contact aureole of the HFC preserve relict mineral assemblages, mineral zoning and variations in mineral compositions and thus demonstrate disequilibrium. Assemblages representing chemical equilibrium at peak contact metamorphism are considered to have developed only in local mm-scale domains, such as inside the cordierite-spinel knots. Garnet is only in equilibrium with contact assemblages in the pyrope-rich rims, while the resorbed garnets largely retain the composition from the regional metamorphism. This makes the selection of suitable equilibrium mineral compositions delicate and P-T estimation difficult, particularly since garnet is essential for pressure calculation.

However, P-T estimates have been obtained using the compositions of the analysed minerals in assumed local equilibrium within specific domains in each thin section. The compositions used are reported in Table 1 and 2. The spread in calculated results, described below and summarised in Table 3 and Fig. 11, is considerable.

P-T estimates

Estimation of the contact metamorphic P-T condition was performed using assemblages in the cordierite-spinel knots (sample L1) and assemblages associated with matrix garnet (sample L1), as well as assemblages associated with the high-Mg garnet rims (sample 2A). The spreadsheet software GPT (Reche & Martinez 1996) was used in the calculations. This software contains a large number of different P-T calibrations for metamorphic assemblages in pelitic rocks, some of which have been used, see below.

For the cordierite-spinel assemblages, T calculations using the garnet-cordierite (GC) and cordierite-spinel (CS) exchange thermometers have been applied, calibrated by Holdaway & Lee (1977) and Vielzeuf (1983),

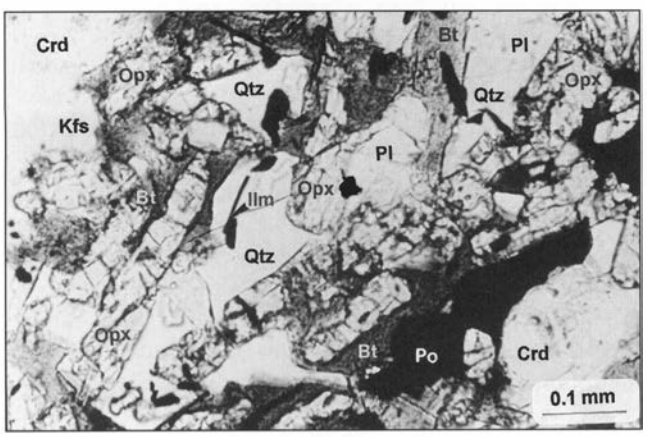

Fig. 9. Photomicrograph of an orthopyroxene (Opx)-rich domain in sample L1. Orthopyroxene replaces biotite (Bt). Other phases present are plagioclase (Pl), quartz (Qzt), K-feldspar (Kfs), cordierite (Crd), ilmenite (Ilm), and pyrrhotite (Po). Plane-polarised light.

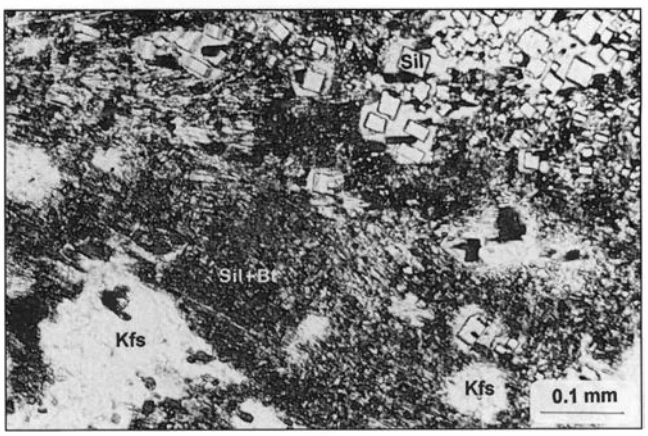

Fig. 10. Photomicrograph showing a domain of fibrolitic and prismatic sillimanite (Sil) intergrown with K-feldspar (Kfs) and biotite (Bt). Light areas around the prismatic grains are K-feldspar. Plane-polarised light. Sample 92046.

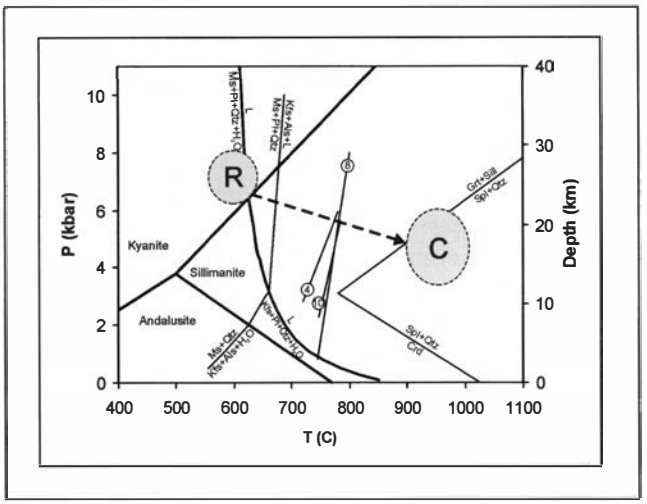

Fig. 11. P-T diagram illustrating the indicated conditions for the HFC contact metamorphism (field C) as determined in this study. The approximate P-T conditions of the preceding Sveconorwegian regional metamorphism (Austin Hegardt 2000) are also shown (field R). Al-silicate stability fields are from Holdaway (1971); the stability field for low Zn-spinel + quartz is after Montel et al. (1986). Muscovite and K-feldspar melting reactions, as well as reactions (4) and (10) are after Pattison & Tracy (1991), while reaction (8) is after Clemens & Wall (1981).

respectively. Although strictly not applicable to the quartz-undersaturated conditions in the cordierite-spinel knots, pressures were calculated from the garnet-cordierite-aluminum silicate (sillimanite)-quartz (GCAQ; Holdaway & Lee 1977) and garnet-plagioclase-aluminum silicate-quartz (GPAQ; Hodges & Crowley 1985) net-transfer reaction barometers for comparative purposes.

The composition of matrix phases in sample L1 and 2A, judged to be in local textural equilibrium with the matrix garnet and pyrope-rich garnet rims, respectively, were used in the calculations. In addition to the GC and CS thermometers above, the garnet-biotite (GB; Holdaway & Lee 1977) and garnet-orthopyroxene (GO; Bhattacharya et al. 1991) thermometers were used. For P estimates, the garnet-plagioclase-biotite-quartz (GPBQ; Hoisch 1990) and garnet-orthopyroxene-plagioclase-quartz (GOPQ; Bhattacharya et al. 1991) barometers were applied.

Contact metamorphism. – Calculations on two separate cordierite-spinel knots give variable results. The first one yields: 886°C (GC) at 3.6 kbar (GCAQ) and 892°C (GC) at 4.7 kbar (GPAQ; An_{56}). The CS thermometer gives significantly higher temperature: 958°C at 4.5 kbar (Table 3). 4.5 kbar is used in the temperature calculations as the closest estimate of pressure when an appropriate P calibration not is available. The second knot yields considerably lower temperatures; 774°C (CS) at 4.1 kbar (GCAQ), 768°C (GC) at 2.9 kbar (GPAQ; An_{61}) and 798°C (CS) at 4.5 kbar. The plagioclase composition used is the most An-rich observed in each knot as this is seemed to be in textural equilibrium with the highest-T assemblage. Using a plagioclase composition with 10 mol% lower An-content, which is found at more central positions in the knots, gives ca. 1 kbar higher pressure. The lower T calculated for the second knot is caused by somewhat more Fe-rich compositions of both spinel and cordierite, particularly spinel (Table 2 and 3). As noted previously, the garnets may not be in equilibrium with the contact metamorphic assemblage in the knots as it has to a large degree been consumed (reactions 5) and has a distinctly lower X_{Prp} (11-16%), compared with the pyrope-rich (up to X_{Prp} 29%) porphyroblast rims in sample 2A.

Using compositions of the quartz-containing assemblages in the matrix of sample L1, including the small garnet shown in Fig. 4, results in temperatures around 770°C at 7.1 kbar (GPBQ) and 2.8 kbar (GOPQ; Table 3). Pressures are divergent and temperatures similar to those for the second Crd-Spl knot (Table 3). This assemblage, and some knots, does not represent equilibration at peak contact metamorphic temperature. Apparently, re-adjustment to peak conditions was not evenly recorded by all assemblages in the aureole. Moreover, partial re-equilibration of these relatively fine-grained assemblages upon cooling of the intrusion may have contributed locally. The high-Mg/high-T garnets may also have been consumed according to reactions (5) and (10).

Estimates of the contact metamorphic P-T conditions were also obtained using the rim of the garnet porphyroblast in sample 2A, strongly enriched in pyrope component (X_{Prp} 29.4; Fe# 66.8; Fig. 5b and 6c), interpreted to have formed during maximum T conditions. Other phases used were high-Mg-spinel, high-Fe-cordierite, high-Fe-Ti-biotite, and orthopyroxene, located in the matrix in the vicinity of the garnet and in apparent textural equilibrium with the garnet. The most Ca-rich internal parts of the patchy plagioclase grains (An_{39}) are considered to be in equilibrium at peak conditions, as the more Na-rich plagioclase is interpreted to have crystallized from the melt phase (Fig. 8). Calculated results are: 929°C (GB) at 6.4 kbar (GPBQ), 1016°C (GO) at 3.7 kbar (GOPQ), 934°C (GC) at 4.5 kbar, and 971°C (CS) at 4.5 kbar (Table 3). The GPBQ barometer probably overestimates the pressure since the assemblage cordierite-spinel-corundum is not stable at pressures above 6 kbar (Hensen 1987). The gentle slope (increasing Fe/(Fe+Mg) = decreasing temperature) of the outermost high-temperature plateau in Fig. 6c, records continued garnet growth during the cooling of the intrusion.

We suggest that peak metamorphic conditions in the HFC aureole be most closely approximated by Crd-Spl-

Table 1. Representative microprobe analyses from sample 2A. Matrix assemblage associated to high-Mg garnet rim used for P-T calculations. Garnet core and intermediate zone with inclusions. Garnet (Grt), cordierite (Crd), biotite, (Bt), plagioclase (Pl), spinel (hercynite; Spl), orthopyroxene (Opx), and ilmenite (Ilm). Two plagioclase analyses from one patchy zoned grain in the matrix are given. Analysis 3:4 is the Ca-richer core and is supposed to represent the plagioclase composition in equilibrium with the contact metamorphic assemblage.

Textural position	Grt-rim + matrix								Grt-core		Grt-interm.		
Analysis	B:7:95	D:4:1	3:7	3:4	3:5	3:3	7:2	3:9	C:5:1	5:12	B:7:77	2	7:6
Mineral	Grt	Crd	Bt	Pl (Ca)	Pl (Na)	Opx	Spl	Ilm	Grt	Pl	Grt	Bt	Pl
SiO_2 (wt%)	37.40	48.91	35.99	58.97	61.93	49.88	n.d.	0.03	35.46	54.69	36.59	34.79	62.34
TiO_2	0.14		.d.	4.18	n.d.	n.d.	0.03	0.09	52.28	0.09	n.d.	n.d.	6.36n.d.
Al_2O_3	21.94	32.34	13.87	25.95	24.30	1.48	59.56	0.02	20.89	28.61	20.96	17.43	23.45
FeO	27.72	8.17	20.39	0.10	n.d.	31.51	33.74	42.72	18.17	0.55	26.81	19.46	0.32
MnO	4.33	0.34	0.21	n.d.	n.d.	1.23	1.04	3.51	16.92	n.d.	11.78	0.47	n.d.
MgO	7.75	8.10	11.06	n.d.	n.d.	14.94	5.34	n.d.	0.65	n.d.	2.77	8.22	n.d.
CaO	0.84	0.04	n.d.	7.97	5.50	0.05	0.02	n.d.	6.65	10.93	1.14	n.d.	5.15
Na_2O	0.12	0.28	0.04	6.74	7.87	0.07	n.d.	n.d.	0.01	5.44	n.d.	0.14	8.46
K_2O	n.d.		0.06	8.64	0.19	0.36	n.d.	n.d.	n.d.	n.d.	0.07	n.d.	9.560.10
Cr_2O_3	0.03	n.d.	0.04	n.d.	n.d.	0.05	n.d.	0.13	n.d.	n.d.	n.d.	n.d.	n.d.
ZnO	n.d.		n.d.	n.d.	n.d.	n.d.	0.04	0.21	0.02	n.d.	n.d.	n.d.	n.d.n.d.
Total	00.27	98.24	94.42	99.92	99.96	99.28	100.00	98.71	99.84	100.29	100.05	96.43	99.82
No. of ions on the basis of 24 O		*18 O*	*24 O*	*8 O*		*6 O*	*4 O*	*3 O*	*24 O*	*8 O*	*24 O*		*8 O*
Si	5.857	5.044	6.078	2.634	2.743	1.965			5.844	2.463	5.934	5.753	2.767
Ti	0.016		0.531			0.001	0.002	1.003	0.011			0.791	
Al	4.049	3.931	2.761	1.366	1.269	0.069	1.968	0.001	4.058	1.518	4.006	3.398	1.226
Fe^{2+}	3.631	0.704	2.880	0.004		1.039	0.759	0.912	2.505	0.021	3.637	2.692	0.012
Fe^{3+}							0.030						
Mn	0.575	0.029	0.030			0.041	0.025	0.076	2.363		1.619	0.066	
Mg	1.808	1.245	2.784			0.878	0.223		0.158		0.669	2.027	
Ca	0.140	0.004		0.381	0.261	0.002			1.175	0.528	0.198		0.245
Na	0.036	0.057	0.012	0.584	0.676	0.005			0.004	0.475		0.044	0.728
K		0.008	1.862	0.011	0.021					0.004		2.018	0.006
Cr	0.004					0.001		0.003					
Zn						0.001	0.002						
Σ cations	16.118	11.023	16.944	4.980	4.970	4.002	3.012	1.995	16.118	5.018	16.063	16.788	4.987
Components													
	X_{Alm} 59.00			An 39.09	27.26	Fs 53.00	Fe' 77.33	X_{Hem} 0	X_{Alm} 40.40	An 52.40	X_{Alm} 59.40		An 25.02
	X_{Grs} 2.28			Ab 59.82	70.59	Wo 0.11	Zn' 0.24	X_{Ilm} 0.924	X_{Grs} 18.95	Ab 47.21	X_{Grs} 3.24		Ab 74.41
	X_{Prp} 29.38			Or 1.09	2.15	En 44.80	Mg' 22.67	X_{Gk} 0	X_{Prp} 2.56	Or 0.39	X_{Prp} 10.93		Or 0.57
	X_{Sps} 9.34						Al' 98.49	X_{Py} 0.076	X_{Sps} 38.10		X_{Sps} 26.44		
Fe #	66.76	36.13	50.84			54.19	78.00		94.05		84.45	57.04	

n.d. = not detected. X_{Alm} = 100×Fe/(Fe+Mg+Mn+Ca); X_{Grs} = 100×Ca/(Fe+Mg+Mn+Ca); X_{Pyp} = 100×Mg/(Fe+Mg+Mn+Ca); X_{Sps} = 100×Mn/(Fe+Mg+Mn+Ca); Fe # = 100×Fe/(Fe+Mg); An = 100×Ca/(Ca+Na+K); Ab = 100×Na/(Na+Ca+K), Or = 100×K/(K+Na+Ca); En = 100+Mg/(Fe+Mg+Mn+Ca); Fs = 100+Fe/(Fe+Mg+Mn+Ca); Wo = 100+Ca/(Fe+Mg+Mn+Ca); Fe' = 100+Fe^{2+}/(Fe^{2+}+Mg); Zn' = 100×Zn/(Zn+Fe^{2+}+Mg); Mg' = 100×Mg/(Mg+Fe^{2+}); Al' = 100×Al/(Al+Cr+Fe^{3+}); X_{Hem} = Fe^{3+}; X_{Gk} = Mg; X_{Py} = Mn; X_{Ilm} = 1-(X_{Hem}+X_{Gk}+X_{Py}). For spinel and ilmenite total iron was recalculated to Fe^{3+} and Fe^{2+} following Droop (1987).

Table 2. Representative microprobe analyses of the cordierite-spinel knot assemblage and matrix assemblage in sample L1 used for P-T calculations. Garnet (Grt), cordierite (Crd), biotite, (Bt), plagioclase (Pl), K-feldspar (Kfs), sillimanite (Sil), corundum (Crn), spinel (hercynite; Spl), orthopyroxene (Opx), and ilmenite (Ilm)

Textural position	knot							matrix						
Analysis	trA:5:7	5:10	5:11	5:1	5:11	5:9	5:12	4:1	4:8	4:7	4:10	4:14	4:13	4:12
Mineral	Grt	Crd	Pl	Kfs	Sil	Crn	Spl	Grt	Crd	Bt	Pl	Opx	Spl	Ilm
SiO_2 (wt%)	36.02	46.51	53.07	62.49	35.16	0.02	n.d.	36.08	46.84	34.55	60.52	47.23	n.d.	0.12
TiO_2	0.11	n.d.	n.d.	n.d.	0.04	n.d.	0.25	n.d.	0.02	4.71	n.d.	0.13	0.13	51.88
Al_2O_3	21.26	31.82	28.78	18.80	62.02	99.00	57.15	21.43	32.46	16.56	24.41	3.69	58.39	n.d.
FeO (total)	32.06	11.69	0.12	0.12	1.63[a]	0.75[a]	37.93	31.82	10.04	20.91	0.03	33.99	36.84	44.57
MnO	4.34	0.76	n.d.	n.d.	0.04	n.d.	0.81	4.12	0.45	0.17	n.d.	1.65	0.51	1.74
MgO	4.07	5.82	n.d.	n.d.	0.29	0.02	2.93	4.46	7.48	8.58	n.d.	12.15	3.34	0.14
CaO	1.21	0.04	11.77	0.25	0.03	n.d.	0.05	1.24	0.06	n.d.	6.43	0.18	n.d.	n.d.
Na_2O	0.01	0.06	5.01	2.74	0.14	n.d.	n.d..	n.d.	0.18	0.04	7.58	n.d.	n.d.	n.d.
K2O	n.d.	n.d.	0.19	11.77	n.d.	n.d.	n.d.	n.d.	n.d.	8.61	0.32	n.d.	n.d.	n.d.
Cr_2O_3	n.d.	n.d.	n.d.	n.d.	n.d.	0.03	0.01	0.04	0.01	0.15	n.d.	n.d.	0.02	0.08
ZnO	n.d.	n.d.	n.d.	n.d.	n.d.	n.d.	0.32	n.d.	0.07	n.d.	n.d.	0.03	0.76	n.d.
Total	99.08	96.71	98.94	96.18	99.18	99.82	99.44	99.19	97.61	94.28	99.29	99.05	99.99	98.53
No. of ions on the basis of 24 O		*18 O*	*8 O*		*5 O*	*3 O*	*4 O*	*24 O*	*18 O*	*24 O*	*8 O*	*6 O*	*4 O*	*3 O*
Si	5.855	4.969	2.430	2.962	0.967			5.844	4.923	5.857	2.710	1.898		0.003
Ti	0.013				0.001		0.005		0.001	0.600		0.004	0.003	0.998
Al	4.072	4.006	1.553	1.051	2.010	1.992	1.946	4.090	4.021	3.309	1.288	0.175	1.963	
Fe^{2+}	4.359	1.045	0.005	0.005			0.869	4.310	0.882	2.964	0.001	1.142	0.855	0.953
Fe^{3+}					0.034	0.010	0.045						0.021	
Mn	0.597	0.069			0.001		0.020	0.566	0.040	0.025		0.056	0.012	0.038
Mg	0.987	0.926			0.012		0.126	1.077	1.171	2.167		0.728	0.142	0.005
Ca	0.211	0.005	0.577	0.013	0.001		0.002	0.216	0.007		0.308	0.008		
Na	0.004	0.013	0.445	0.252	0.007				0.036	0.013	0.658			
K			0.011	0.712						1.861	0.018			
Cr								0.005		0.020				0.002
Zn							0.004		0.006			0.001	0.009	
∑ cations	16.098	11.034	5.021	4.994	3.032	2.002	3.08	16.108	11.88	16.816	4.984	4.012	3.000	1.999
Components														
	X_{Alm} 70.83		An 55.87	1.33			Fe' 87.35	X_{Alm} 69.88			An 31.31	Fs 59.06	Fe' 85.80 X_{Hem} 0	
	X_{Grs} 3.43		Ab 43.06	25.76			Zn' 0.37	X_{Grs} 3.50			Ab 66.82	Wo 0.40	Zn' 0.85 X_{Ilm} 0.957	
	X_{Prp} 16.04		Or 1.06	72.91			Mg' 12.64	X_{Prp} 17.46			Or 1.87	En 37.63	Mg' 14.20 X_{Gk} 0.005	
	X_{Sps} 9.71						Al' 97.72	X_{Sps} 9.17					Al' 98.90 X_{Py} 0.038	
Fe #	81.53	53.00					87.90	80.01	42.97	57.77		61.08	86.09	

n.d. = not detected. [a] Total Fe as Fe_2O_3 in sillimanite and corundum. X_{Alm} = 100x$Fe/(Fe+Mg+Mn+Ca)$; X_{Grs} = 100x$Ca/(Fe+Mg+Mn+Ca)$; X_{Prp} = 100x$Mg/(Fe+Mg+Mn+Ca)$; X_{Sps} = 100x$Mn/(Fe+Mg+Mn+Ca)$; Fe # = 100x$Fe/(Fe+Mg)$; An = 100x$Ca/(Ca+Na+K)$; Ab = 100x$Na/(Na+Ca+K)$, Or = 100x$K/(K+Na+Ca)$; En = 100x$Mg/(Fe+Mg+Mn+Ca)$; Fs = 100x$Fe/(Fe+Mg+Mn+Ca)$; Wo = 100x$Ca/(Fe+Mg+Mn+Ca)$; Fe' = 100x$Fe^{2+}/(Fe^{2+}+Mg)$; Zn' = 100x$Zn/(Zn+Fe^{2+}+Mg)$; Mg' = 100x$Mg/(Mg+Fe^{2+})$; Al' = 100x$Al/(Al+Cr+Fe^{3+})$; $X_{Hem} = Fe^{3+}$; $X_{Gk} = Mg$; $X_{Py} = Mn$; $X_{Ilm} = 1-(X_{Hem}+X_{Gk}+X_{Py})$. For spinel and ilmenite total iron was recalculated to Fe^{3+} and Fe^{2+} following Droop (1987).

Table 3. P-T estimates for the HFC contact metamorphism. Thermometers used are garnet-cordierite (GC), garnet-orthopyroxene (GO), garnet-biotite (GB), and cordierite-spinel (CS); barometers used are garnet-orthopyroxene-plagioclase-quartz (GOPQ), garnet-cordierite-aluminum silicate-quartz (GCAQ), garnet-plagioclase- aluminum silicate-quartz (GPAQ), and garnet-plagioclase-biotite-quartz (GPBQ). Mineral compositions are displayed by Fe# (100xFe/(Fe+Mg) except plagioclase which show An-content, full analyses are given in Table 1 and 2. Bold numbers are suggested to represent the best estimate of the contact metamorphic condition. A pressure of 4.5 kbar is used in the temperature calculations as the closest estimate of pressure when an appropriate P calibration not is available. Numbers within parenthesis are reported for comparison but should not be regarded as reliable values since quartz is not stable in the Crd-Spl knots and sillimanite is not stable in the matrix and at the pyrope-rich Grt-rim. Concerning calculations for 2A Grt intermediate zone, the results should not be regarded as true values but as the best estimate for the regional metamorphism from these samples. See text for discussion.

	Thermometers (°C)				Barometers (kbar)			
Sample	GC	GO	GB	CS	GOPQ	GCAQ	GPAQ	GPBQ
L1, Crd-Spl knot (Grt 82, Crd 53, Pl 56, Spl 88)	886			958		(3.6)	(4.7)	
L1, Crd-Spl knot (Grt 87, Crd 57, Pl 61, Spl 91)	774			798		(4.1)	(2.9)	
L1, matrix (Grt 80, Crd 43, Bt 58, Pl 31, Opx 61, Spl 86)	775	774	770	764	2.8	(4.9)	(5.9)	7.1
2A, Grt rim (Grt 67, Crd 36, Bt 51, Pl 39, Opx 54, Spl 78)	934	1016	929	971	3.7	(4.5)	(5.2)	6.4
2A, Grt intermediate zone (Grt 85, Bt 57, Pl 19)			(654)					(6.9)

Opx-Pl ± Bt assemblages in local equilibrium with the most pyrope-rich garnet rims, and by local equilibrium in some SiO_2-undersaturated cordierite-spinel knots. Thermometers, including GB, GC, CS and, GO applied to these assemblages varies from ca. 890 to 1015°C (Table 3). This is supported by the fact that complete elimination of biotite in quartz-undersaturated domains of metapelitic rocks, such as in the cordierite-spinel knots, indicate temperatures above 900°C (Sengupta et al. 1999), which is in accordance with two-pyroxene crystallisation temperatures of 1040° to 1080° C determined for the HFC norite (Årebäck & Stigh 2000). Pressure calculations using GOPQ and GPBQ indicate conditions in the range of 3.7 to 6.4 kbar.

P-T estimates from the coeval late Sveconorwegian contact aureole around the 930 Ma Rogaland anorthosite complex in SW Norway (Schärer et al. 1996) have yielded 4-7 kbar and up to 1050°C (Wilmart & Duchesne 1987; Jansen et al. 1985; Tobi et al. 1985; Wilmart et al. 1991). Experimental phase equilibrium data from the Bjerkreim-Sokndal layered intrusion, belonging to the Rogaland anorthosite complex, indicate an emplacement pressure of ≤ 5 kbar (Van der Auwera & Longhi 1994). Contact metamorphic assemblages in xenoliths of the late Sveconorwegian 920 Ma Bohus granite (Eliasson & Schöberg 1991), emplaced ca. 40 km north of HFC indicate pressures of about 4 kbar and temperatures around 715°C, corresponding to a depth of ca. 14 km (Eliasson et al., in prep.).

Regional metamorphism. – Except for the cores and intermediate zones in porphyroblastic garnet, minerals are likely to have recorded prograde and retrograde contact-metamorphic conditions. However, garnet zoning indicates that there were two episodes of garnet growth prior to intrusion of the HFC. Hence, the garnet zoning appears to record three metamorphic episodes, where the inner, inclusion-poor core (commonly lacking) represents an early stage, and the surrounding, inclusion-rich intermediate zone a later stage of regional metamorphism. The zoning in the intermediate zone (steady decrease in Fe/(Fe+Mg)) suggests prograde growth, ending with a sudden strong increase in temperature during the growth of the inclusion-free rim at the time of HFC intrusion. The prograde zoning in the intermediate zone is interpreted to have developed during a Sveconorwegian regional event, preceding

emplacement of the HFC. The development of the high X_{Grs} cores could be related to a pre-Sveconorwegian event, although this is unknown at present.

The considerable variation in composition of the plagioclase inclusions in the porphyroblastic garnet and the fact that only two biotite inclusions (of which one was chloritised) were found in the porphyroblastic garnet, makes regional metamorphic P-T estimation in these samples very tentative. However, in Table 3 one calculation is reported using garnet, plagioclase and biotite from the intermediate zone in a garnet porphyroblast. The result, about 650°C at 7 kbar, is in good agreement with previous P-T estimates from SLM rocks (Austin Hegardt 2000; Sigurdsson 1990), but should be regarded as provisional. More petrologic work is needed for reconstruction of the regional P-T evolution in the SLM and the Western Segment.

Conclusions

Petrographic examination of rocks from the contact aureole of the HFC shows that the pre-existing SLM amphibolite-facies assemblage (quartz, plagioclase, biotite, muscovite, K-feldspar and garnet) has been strongly affected by the contact metamorphism. Biotite, quartz, plagioclase and garnet were partially consumed, while muscovite disappeared completely. Newly formed contact metamorphic minerals comprise sillimanite, cordierite, orthopyroxene, corundum, high-T garnet rims, and hercynitic spinel, as well as new formation of K-feldspar and melt (Kfs+Qtz+Na-rich Pl). Remaining biotite and plagioclase underwent considerable compositional changes. A particular feature is the intergrowths of cordierite and spinel, forming SiO_2-undersaturated knots, including also sillimanite, corundum, plagioclase and K-feldspar.

There is abundant evidence of disequilibrium, both texturally and chemically. Plagioclase is strongly patchily zoned, where low-An marginal areas represent late plagioclase precipitated from melt. Garnet preserves pre-intrusive growth zoning, and show both high-T growth and resorption. This, in addition to significant chemical variation for most minerals, suggests partial equilibrium or non-equilibrium rather than true chemical equilibrium.

Estimated peak metamorphic conditions from local equilibrium or near-equilibrium assemblages vary from 3.7 to 6.4 kbar and 890 to 1015°C, corresponding to low-P ultra-high temperature granulite-facies. The coexistence of cordierite + spinel + corundum suggest an upper limit for the pressure of ca. 6 kbar, i.e. maximum 21-22 km depth in the crust (Hensen 1987). The values obtained here are close to those obtained for the contemporaneously intruded, but much larger Rogaland anorthosite complex (e.g. Jansen et al. 1985; Schumacher & Westphal 2001), and would roughly correspond to an uplift of ca. 5-10 km between the regional metamorphic event and the HFC intrusion in the area, which could have been accomplished in the late Sveconorwegian (cf. Jansen et al. 1985).

Acknowledgements. – Hans Harryson is thanked for technical assistance with the microprobe analyses at Uppsala University. D. Cornell made valuable comments on the manuscript. Journal reviews by M. Westphal, J. Schumacher, and in particular C. Möller substantially improved the paper. The second author acknowledges a postdoc grant from STINT (Stiftelsen för internationalisering av högre utbildning och forskning).

References

Åhäll, K.-I., Daly, J.S. & Schöberg, H. 1990: Geochronological constraints on mid Proterozoic magmatism in the Östfold-Marstrand Belt: implications for crustal evolution in southwest Sweden. In Gower, C.F., Rivers, T. & Ryan, B. (eds.): *Mid-Proterozoic Laurentia-Baltica,* 97-115. Geological Association of Canada Special Paper 38.

Åhäll, K.-I., Cornell, D.H. & Armstrong, R. 1998: Ion probe dating of meta-sedimentary units across the Skagerrak: new constraints for early Mesoproterozoic growth of the Baltic Shield. *Precambrian Research 87,* 117-134.

Ahlin, S. 1976: The compositional relationships of biotite and garnet in the Göteborg area southwestern Sweden, and their thermometric implications. *Geologiska Föreningens i Stockholm Förhandlingar 98,* 337-342.

Andersson, U.B., Larsson, L. & Wikström, A. 1992: Charnockites, pyroxene granulites, and garnet-cordierite gneiss at a boundary between early Svecofennian rocks and Småland-Värmland granitoids, Karlskoga, southern Sweden. *Geologiska Föreningens i Stockholm Förhandlingar 114,* 1-15.

Årebäck, H. 1995: *The Hakefjorden Complex - geology and petrogenesis of a late Sveconorwegian norite-anorthosite intrusion, south-west Sweden.* Unpublished Ph.Lic. thesis, Earth Sciences Centre, Göteborg University, A9.

Årebäck, H. 2001: *Petrography, geochemistry and geochronology of mafic to intermediate late Sveconorwegian intrusions: the Hakefjorden Complex and Vinga intrusion, SW Sweden.* Unpublished Ph.D. thesis, Earth Sciences Centre, Göteborg University, A72.

Årebäck, H. & Stigh, J. 1997: Polybaric evolution of the Hakefjorden Complex, southwestern Sweden, deduced from partial dissolution in andesine megacrysts. *Geologiska Föreningens i Stockholm Förhandlingar 119,* 97.101.

Årebäck, H. & Stigh, J. 2000: Nature and origin of an anorthosite associated ilmenite-rich leuconorite, Hakefjorden Complex, SW Sweden. *Lithos 51,* 247-267.

Austin Hegardt, E. 2000: *A Sveconorwegian crustal subduction and exhumation model for the Eastern Segment, south-western Sweden.* Unpublished M.Sc thesis, Earth Science Centre, Göteborgs University, B220, 38 pp.

Bhattacharya, A., Krishnakumar, K.R., Raith, M. & Sen, S.K. 1991: An improved set of a-X parameters for Fe-Mg-Ca garnets and refinements of the orthopyroxene-garnet thermometer and the orthopyroxene-garnet-plagioclase-quartz barometer. *Journal of Petrology 32,* 629-656.

Bégin, N.J. & Pattison, D.R.M. 1994: Metamorphic evolution of granulites in the Minto Block, northern Québec: extraction of peak P-T conditions taking account of late Fe-Mg exchange. *Journal of Metamorphic Geology 12,* 411-428.

Berg, J.H. 1977: Dry granulite mineral assemblages in the contact aureoles of the Nain complex, Labarador. *Contributions to Mineralogy and Petrology 64,* 33-52.

Bergström, L. 1963: Petrology of the Tjörn area in western Sweden. *Sveriges Geologiska Undersökning C 593,* 134 pp.

Bucher, K. & Frey, M. 1994: *Petrogenesis of metamorphic rocks. 6:th complete revision of Winkler's textbook.* Springer-Verlag, Berlin, 318 pp.

Clarke, G.L., Collins, W.J. & Vernon, R.H. 1990: Successive overprinting granulite facies metamorphic events in the Anmatjira Ranges, central Australia. *Journal of Metamorphic Geology 8,* 65-88.

Clemens, J.D. & Wall, V.J. 1981: Origin and crystallization of some peraluminous (S-type) granitic magmas. *Canadian Mineralogist 19,* 111-131.

Cornell, D.H., Årebäck, H. & Scherstén, A. 2000: Ion microprobe discovery of Archaean and Early Proterozoic zircon xenocrysts in southwest Sweden. *Geologiska Föreningens i Stockholm Förhandlingar 122,* 377-383.

Dasgupta, S., Ehl, J., Raith, M., Sengupta, P. & Sengupta, Pr. 1997: Mid-crustal contact metamorphism around the Chima-Kurthy mafic-ultramafic complex, eastern Ghats Belt, India. *Contributions to Mineralogy and Petrology 129,* 182-197.

Dietvorst, E.J.L. 1980: Biotite breakdown and the formation of gahnite in metapelitic rocks from Kemiö, southwest Finland. *Contributions to Mineralogy and Petrology 75,* 327-337.

Droop, G.T.R. 1987: A general equation of estimating Fe^{3}+ concentrations in ferromagnesian silicates and oxides from microprobe analyses, using stoichiometric criteria. *Mineralogical Magazine 51,* 431-435.

(Eliasson, T., Ahlin, S. & Petersson, J. in prep.: Emplacement mechanism and thermobarometry of the Sveconorwegian Bohus granite, SW Sweden.)

Fitzsimons, I.C.W. 1996: Metapelitic migmatites from Brattstrand Bluffs, east Antarctica – metamorphism, melting and exhumation of the mid crust. *Journal of Petrology 37,* 395-414.

Grant, J.A. & Frost, B.R. 1990: Contact metamorphism and partial melting of pelitic rocks in the aureole of the Laramie anorthosite complex, Morton Pass, Wyoming. *American Journal of Science 290,* 425-472.

Harley, S.L. 1996: On the occurrence and characterization of ultra-high-temperature crustal metamorphism. *In* Treloar, P.J. & O'Brien, P.J. (eds.): *What drives metamorphism and metamorphic reactions,* 81-107. Geological Society, Special Publication 138.

Hensen, B.J. 1987: P-T grids for silica-undersaturated granulites in the system MAS (n+4) and FMAS (n+3) – tools for derivation of P-T paths of metamorphism. *Journal of Metamorphic Geology 5,* 255-271.

Hodges, K.V. & Crowley, P.D. 1985: Error estimation and empirical geothermobarometry for pelitic systems. *American Mineralogist 70,* 702-709.

Hoisch, D. 1990: Empirical calibration of six geobarometers for the mineral assemblage quartz+muscovite+biotite+plagioclase+garnet. *Contributions to Mineralogy and Petrology 104,* 225-234.

Holdaway, M.J. 1971: Stability of andalusite and aluminium silicate phase diagram. *American Journal of Science 271,* 97-131.

Holdaway, M.J. & Lee, S.M. 1977: Fe-Mg cordierite stability in high-grade pelitic rocks based on experimental, theoretical, and natural observations. *Contributions to Mineralogy and Petrology 63,* 175-198.

Jansen, J.B.H, Blok, R.J.P, Bos, A. & Scheelings, M. 1985: Geothermometry and geobarometry in Rogaland and preliminary results from the Bamble area, S. Norway. In Tobi, A.C. & Touret, J.L.R. (eds.): *The deep Proterozoic crust in the North Atlantic provinces,* 499-516. Reidel Publication.

Li, C. & Naldrett, A.J. 2000: Melting reactions of gneissic inclusions with enclosing magma at Voisey's Bay, Labrador, Canada: Implications with respect to ore genesis. *Economic Geology 95,* 810-814.

Loomis, T.P. 1972: Contact metamorphism of pelitic rock by the Ronda ultramafic intrusion, southern Spain: *Geological Society of America Bulletin 83,* 2449-2474.

Magnusson, N.H. 1960: Age determinations of Swedish Precambrian rocks. *Geologiska Föreningens i Stockholm Förhandlingar 82,* 407-432.

Montel, J.-M., Weber, C. & Pichavant, M. 1986: Biotite-sillimanite-spinel assemblages in high-grade metamorphic rocks: Occurrences, chemographic analysis and thermobarometric interest. *Bulletin Minéralogique 109,* 555-573.

Owen, J.V. 1991: Cordierite+spinel paragenesis in pelitic gneiss from contact aureoles of the Mistastin batholith (Québec) and the Taylor Brook gabbro complex (Newfoundland). *Canadian Journal of Earth Science 28,* 372-381.

Pattison, D.R.M. & Tracy, R.J. 1991: Phase equilibria and thermobarometry of metapelites. *In* Kerrick, D.M. (ed.): *Contact Metamorphism,* 105-206. American Mineralogical Society of America, Reviews in Mineralogy 26.

Reche, J. & Martinez, F.J. 1996: GPT: An excel spreadsheet for thermobarometric calculations in metapelitic rocks. *Computers & Geosciences 22,* 775-784.

Schärer, U., Wilmart, E & Duchesne, J.C. 1996: The short duration and anorogenic character of anorthosite magmatism: U-Pb dating of the Rogaland complex, Norway. *Earth and Planetary Science Letters 139,* 335-350.

Scherstén, A., Årebäck, H., Cornell, D.H., Hoskin, P., Åberg, A. & Armstrong, R. 2000: Dating mafic-ultramafic intrusions by ion-probing contact-melt zircon: examples from SW Sweden. *Contributions to Mineralogy and Petrology 139,* 115-125.

Schumacher, J.C. & Westphal, M. 2001: Thermal modelling of the metamorphism of the Rogaland granulites. *In* Korneliussen, A. (ed.): Abstracts – *GEODE field workshop 8-12th July 2001 on ilmenite deposits in the Rogaland anorthosite province, S. Norway.* Norges geologiske undersøkelse Report 2001.042, 127-128.

Scrimgeour, I., Smith, J.B. & Raith, J.G. 2001: Palaeoproterozoic high-T, low-P metamorphism and dehydration melting in metapelites from the Mopunga Range, Arunta Inlier, central Australia. *Journal of Metamorphic Geology 19,* 739-757.

Sengupta, P., Sen, J., Dasgupta, S., Raith, M., Bhui, U.K. & Ehl, J. 1999: Ultra-high temperature metamorphism of metapelitic granulites from Kondapalle, eastern Ghats belt: implications for the Indo-Antarctic Correlation. *Journal of Petrology 40,* 1065-1087.

Sigurdsson, O.B. 1990: The Stora Le-Marstrand formation, SW Sweden; metamorphic and petrographic relationship. *Geologiska Föreningens i Stockholm Förhandlingar 112,* 302-303.

Srogi, L., Wagner, M.E. & Lutz, T.M. 1993: Dehydration partial melting and disequilibrium in granulite-facies Wilmington Complex, Pennsylvania-Delaware Piedmont. *American Journal of Science 293,* 405-462.

Tobi, A.C., Hermans, G.A.E.M., Maijer, C. & Jansen, J.B.H., 1985: Metamorphic zoning in the high-grade Proterozoic of Rogaland-Vest Agder, SW Norway. *In* Tobi, A.C. & Touret, J.L.R. (eds.): *The deep Proterozoic crust in the North Atlantic Provinces,* 477-497. Reidel Publication.

Van der Auwera, J. & Longhi, J. 1994: Experimental study of a jotunite (hypersthene monzodiorite): constraints on the parent magma composition and crystallisation conditions (P, T, f_{O2}) of the Bjerkreim-Sokndal layered intrusion (Norway). *Contributions to Mineralogy and Petrology 118,* 60-78.

Vielzeuf, D. 1983: The Spinel and quartz associations in high grade xenoliths from Tallanate (S.E. Spain) and their potential use in

geothermometry and barometry. *Contributions to Mineralogy and Petrology 82,* 301-311.

Waters, D.J. 1988: Partial melting and the formation of granulite facies assemblages in Namaqualand, South Africa. *Journal of Metamorphic Geology 6,* 387-404.

Waters, D.J. 1991: Hercynite-quartz granulites: phase relations, and implications for crustal processes. *European Journal of Mineralogy 3,* 367-386.

Whittington, A., Harris, N. & Baker, J. 1998: Low-pressure crustal anatexis: the significance of spinel and cordierite from metapelitic assemblages at Nanga Parbat, northern Pakistan. *In* Treloar, P.J. & O'Brien, P.J. (eds.): *What drives metamorphism and metamorphic reactions?,* 183-198. Geological Society, London, Special Publications, 138.

Wilmart, E. & Duchesne, J.C. 1987: Geothermobarometry of igneous and metamorphic rocks around the Åna-Sira anorthosite massif: implications for the depth of emplacement of the south Norwegian anorthosites. *Norsk Geologisk Tidsskrift 67,* 185-196.

Wilmart, E., Clocchiatti, R., Duchesne, J.C. & Touret, J.L.R. 1991: Fluid inclusions in charnockites from the Bjerkreim-Sokndal massif (Rogaland, southwestern Norway): fluid origin and in situ evolution. *Contributions to Mineralogy and Petrology 108,* 453-462.